

Simulation of Magnetic Island Dynamics under RMP with the TEAR Code and Validation of the Results on T-10 Tokamak Data

N.V. Ivanov, A.M. Kakurin

National Research Centre «Kurchatov Institute», Moscow, Russia

The experimental validation of the TEAR code against the T-10 tokamak data on the $m = 2$ mode behavior under RMP is presented. The Ohmic regime with the intrinsically rotating $m = 2$ mode is chosen for the code validation. The RMP consists of the stationary error field, the magnetic field of the eddy current in the resistive vacuum vessel wall and the magnetic field of the externally applied controlled halo-current in the plasma SOL [1 - 4].

The halo-current loop consists of the rail limiter, plasma SOL, vacuum vessel and external part of the circuit. The angular position of the $m = 2, n = 1$ component of the halo-current magnetic field coincides within ten degrees with the position of the same component of the error field. In two options, a controllable connector or a controllable EMF source are introduced into the external part of the halo-current circuit. A capacitor bank is used as the power supply for the EMF source. In separate experiments the EMF source is controlled by two types of signals. In the first case of the preprogrammed control signal, the direct halo-current with different amplitudes and directions or the oscillating halo-current with variable frequency is applied to the originally rotating $m = 2$ mode. In the second case, the control signal is formed by a feedback circuit from the $m = 2$ mode signal of the MHD magnetic sensors.

The space structure of the MHD mode is measured with a set of poloidal magnetic field sensors located at the inner side of the vacuum vessel wall. For each mode with certain poloidal, m , and toroidal, n , numbers the poloidal magnetic field perturbation at the radial position of the magnetic sensors is $B(\theta, \varphi, t) = B_C(t) \cos(m\theta - n\varphi) + B_S(t) \sin(m\theta - n\varphi)$, where φ and θ are the toroidal and poloidal angles respectively, $B_C(t)$ and $B_S(t)$ are the cosine and sine components of the measured mode of the magnetic perturbation. The amplitude of the mode is $B_{\text{AMPL}}(t) = \sqrt{B_C^2(t) + B_S^2(t)}$. The spatial phase of this mode is defined as $\Phi(t) = \arctan[B_S(t)/B_C(t)]$ and the instantaneous value of the mode frequency is $\Omega(t) = d\Phi/dt$. The frequency averaged over period of the oscillations is denoted by $\langle \Omega \rangle$.

The TEAR code [5] is based on the two-fluid MHD approximation that gives coupled diffusion-type equations for the magnetic flux perturbation and for the plasma rotation velocity. The inverse resistive time, $\omega_R = 100 \text{ s}^{-1}$, and the intrinsic value of mode natural frequency, $\Omega_{\text{nat}}/2\pi = 2.5 \text{ kHz}$, are considered as input parameters in our calculations. The cosine and sine components, Δ'_C and Δ'_S , of the tearing mode stability index are found separately for both the cosine and sine space components of the flux function. In the calculations of the flux function radial dependences, we take into account the halo-current at the plasma boundary with the surface density calculated according to [4] and two currents outside the plasma, including the current which produces the error field and the current generated in the resistive vacuum vessel wall due to the magnetic flux variations in time.

We consider the axisymmetric velocities of the toroidal and poloidal plasma rotation. The values of plasma viscosity components are chosen under the assumptions that the Prandtl number [6] can be of the order of unity or a few times exceed unity and that the poloidal viscosity is much higher than the toroidal viscosity. Under these assumptions, the values of the toroidal and poloidal momentum radial diffusivity $\mu_\phi/\rho = (0.6 \div 0.8) \text{ m}^2\text{s}^{-1}$ and $\mu_\theta/\mu_\phi = 200$ are used in the calculations.

Halo-current induced by the rotating $m = 2, n = 1$ mode

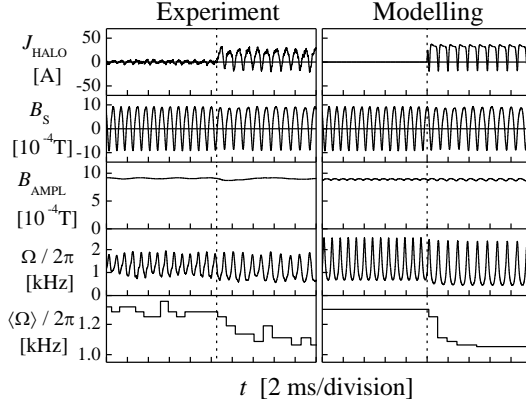


FIG.1. The effect of the induced halo-current on the $m = 2$ mode rotation. The switching time of the controlled connector is shown with the vertical dashed lines.

magnetic field. The experimentally obtained current-voltage characteristic of this circuit is used in the calculations.

In this experiment [1], the external part of the halo-current circuit between the rail limiter and vacuum vessel is provided with a controllable connector that is switched on at a preprogrammed moment of time during the tokamak discharge. After the connector is switched on, an oscillating current arises in the halo-current circuit. The switching-on of the connector in the halo-current circuit results in a downshift of the MHD mode frequency. This result is illustrated in the left panel of FIG.1. The result of simulation is shown in the right panel of the same figure. The halo-current is calculated as the current induced in the halo-current circuit by the oscillating $m = 2$ mode

frequency. The result of simulation is shown in the right panel of the same figure. The halo-current is calculated as the current induced in the halo-current circuit by the oscillating $m = 2$ mode

Preprogrammed direct halo-current pulse

The experimental waveforms of the halo-current and the $m = 2$ mode signals are shown in the left panels of FIG.2, FIG.3 and FIG.4 for cases of different halo-current directions and amplitudes. In these figures one can see that the direct halo-current affects the instantaneous value of the mode frequency. The mode rotation stops in cases of high amplitude halo-current pulses. This mode-locking effect has different threshold values at the positive (FIG.2) and negative (FIG.3) halo-current directions.

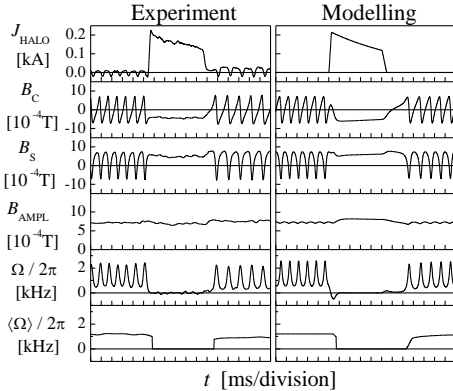


FIG.2. The $m = 2$ mode locking by the positive halo-current pulse

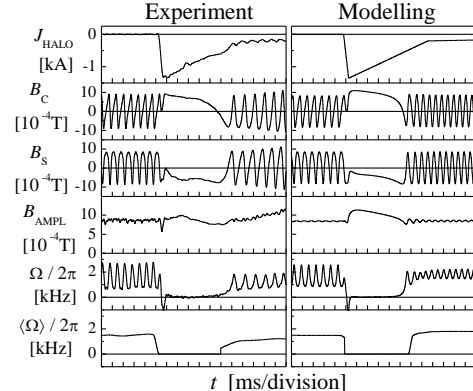


FIG.3. The $m = 2$ mode locking by the negative halo-current pulse

For the moderate halo-current amplitude (see FIG.4), the effect on the mode rotation depends on the halo-current direction. The application of the negative halo-current is followed by an increase of the mode frequency. After the change of the halo-current sign to positive, the mode frequency decreases and the mode rotation becomes more irregular.

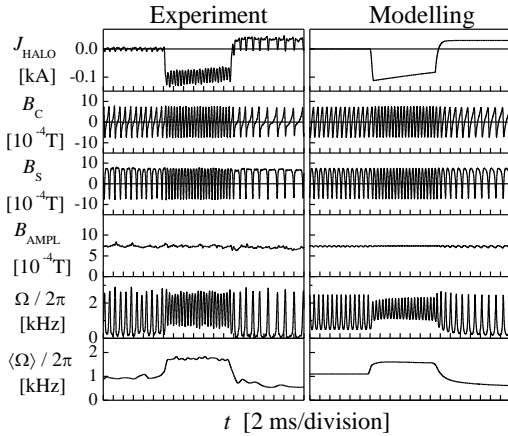


FIG.4. The effect of the moderate direct halo-current on the $m = 2$ mode rotation
negative halo-current takes place. In the case of the positive halo-current, its magnetic field is added to the error field.

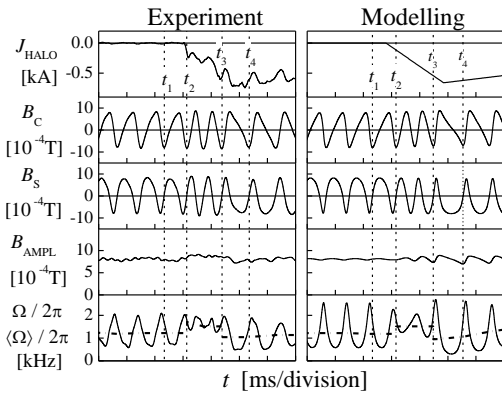


FIG.5. The $m = 2$ mode dynamics under the direct halo-current variation in time. The average frequency is shown with dash-dot curves in the bottom panels.

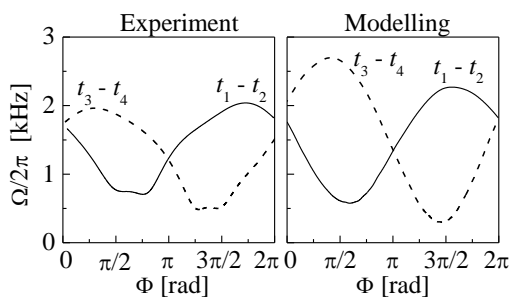


FIG.6. The dependences of the $m = 2$ mode instantaneous frequency on the current value of the mode phase in two time intervals $(t_1 - t_2)$ and $(t_3 - t_4)$ shown with vertical dashed lines in FIG.5

$m = 2$ mode frequency follows the halo-current frequency Ω_{HALO} . This result is illustrated in FIG.7, where the case of a saw-tooth-form variation of the control signal frequency is shown.

In the cases of preprogrammed halo-current, the waveforms of its pulses are used as input data for our calculations. The results of the simulation are shown in the right panels of FIG.2, FIG.3 and FIG.4. Similar to the experiment, the changes of the mode dynamics are attributed to the joint effect of the permanent error field and the magnetic field of the applied halo-current. In the case of positive halo-current, the mode locking takes place at lower halo-current amplitude because in this case the error field and the magnetic field of halo-current have same directions. In FIG. 4, a partial compensation of the error field by the magnetic field of the

The experimental data and simulation results on the process of the halo-current relatively slow variation in time are shown in FIG.5. In this figure one can see the variation of the halo-current value from zero to minus 0.7 kA during several oscillation periods. Along with the halo-current variation, the total value of RMP consisting of the error field and magnetic field of the halo-current first decreases to zero and then increases in the opposite direction. In this process, the range of the instantaneous frequency fluctuations decreases and later increases again. The transition of RMP through the zero value is accompanied by the change of the mode instantaneous frequency dependence on the current value of the mode spatial phase (FIG.6).

The observed fluctuations of the mode rotation velocity take place due to cyclical variations of the electromagnetic torque applied to the resonant layer in the process of magnetic island rotation with respect to the RMP. The phase of these fluctuations depends on the RMP direction.

Preprogrammed oscillating halo-current

Under the oscillating control signal, the shift of the $m = 2$ mode frequency to the value of the halo-current frequency is observed [2]. In the case of the control signal frequency variation, the

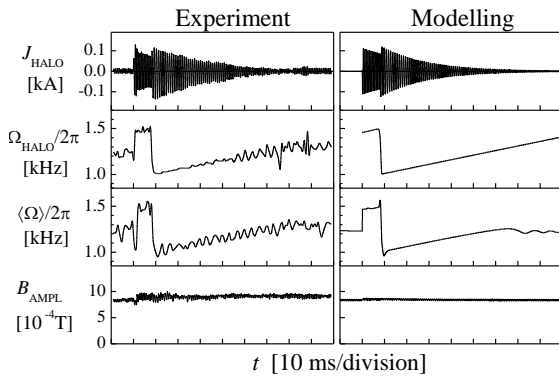


FIG.7. The $m = 2$ mode dynamics under halo-current frequency variation

frequency under feedback-controlled halo-current are observed in this experiment. Similar frequency variations take place in the modelling of this experiment shown in the right panels of FIG.8 and FIG.9.

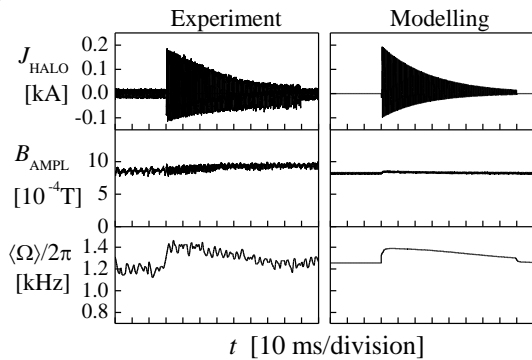


FIG.8. Variation of the $m = 2$ mode frequency under feedback-controlled halo-current:

$$J_{\text{HALO}} = K_{\text{FB}} dB_S/dt$$

Feedback-controlled halo-current

In this experiment [2], the time derivative of the $m = 2$ mode sine component is used as the feedback signal to control the halo-current. The effect of the halo-current on the mode dynamics depends on the choice of the feedback phase shift (see FIG.8 and FIG.9). The absolute value of the feedback gain, K_{FB} , is 24 AsT^{-1} just after the switching-on of the EMF power supply and degrades to zero along with the discharge of the power supply capacitor. Some variations of the mode

frequency are observed in this experiment. Similar

frequency variations take place in the modelling of this experiment shown in the right

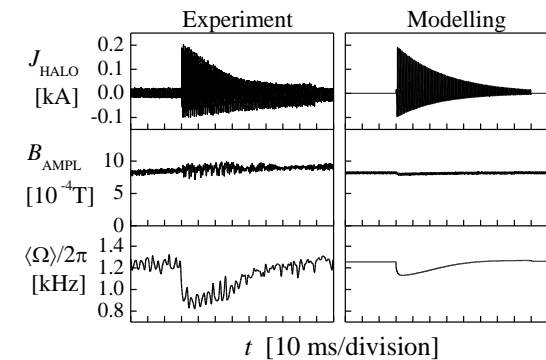


FIG.9. Variation of the $m = 2$ mode frequency under feedback-controlled halo-current:

$$J_{\text{HALO}} = -K_{\text{FB}} dB_S/dt$$

Summary

A good agreement is obtained between the results of the TEAR code calculations and experimental data on the tearing mode behavior under resonant magnetic perturbation in T-10 tokamak. The magnetic field of the controlled halo-current in the plasma SOL is included in the RMP. In the experiment and modelling, a downshift of the mode frequency is observed under halo-current induced by rotating $m = 2$ mode. In the case of the preprogrammed halo-current control signal, the rotation of the $m = 2$ mode stops under a sufficiently high pulse of direct halo-current. The application of an oscillating halo-current results in the shift of the $m = 2$ mode frequency to the frequency of the halo-current oscillations. In the case of the feedback control, some increase or decrease of the $m = 2$ mode frequency are observed at different values of the feedback phase shift.

- [1] Ivanov N.V., et al. 18th IAEA FEC, Sorrento, Italy (2000) IAEA-CN-77/EXP2/02.
- [2] Chudnovskiy A.N., et al. Nucl. Fusion (2003) **43**, p. 681.
- [3] Ivanov N.V., et al. 32nd EPS Conf. on Plasma Physics and Controlled Fusion (2005) P-5.068: http://epsppd.epfl.ch/Tarragona/pdf/P5_068.pdf
- [4] Ivanov N.V. and Kakurin A.M. Plasma Physics Reports (2011) **37**, p. 28.
- [5] Ivanov N.V., Kakurin A.M., Konovalov S.V. 24th IAEA FEC (2012) TH/P3-22: http://www-naweb.iaea.org/napc/physics/FEC/FEC2012/papers/342_THP322.pdf; PAS&T/TF (2013) **36**, 2, p. 55: http://vant.iterru.ru/vant_2013_2/6.pdf
- [6] Tala T. et al. Nucl. Fusion (2011) **51**, 123002.